Biochimica et Biophysica Acta 1794 (2009) 1159–1167

Contents lists available at ScienceDirect

Biochimica et Biophysica Acta

journal homepage: www.elsevier.com/locate/bbapap

A flexible loop controlling the enzymatic activity and specificity in a glycosyl hydrolase family 19 endochitinase from barley seeds (*Hordeum vulgare* L.)

Tamo Fukamizo [a,*], Ryoh Miyake [a], Atsushi Tamura [a], Takayuki Ohnuma [a], Karen Skriver [b], Niko V. Pursiainen [c], André H. Juffer [c]

[a] Department of Advanced Bioscience, Kinki University, Nara 631-8505, Japan
[b] Department of Biology, University of Copenhagen, Universitetsparken 2100, Copenhagen, Denmark
[c] The Biocenter Oulu and Department of Biochemistry, University of Oulu, PO Box 3000, Oulu, Finland

ARTICLE INFO

Article history:
Received 19 December 2008
Received in revised form 12 March 2009
Accepted 13 March 2009
Available online 28 March 2009

Keywords:
Chitinase
Barley seed
Tryptophan residue
Substrate binding
Anomeric selectivity

ABSTRACT

To examine the role of the loop structure consisting of residues 70–82 (70–82 loop) localized to +3/4 subsite of the substrate binding cleft of a family GH-19 endochitinase from barley seeds, Trp72 and Trp82 were mutated, and the mutated enzymes (W72A, W82A, and W72A/W82A) were characterized. Thermal stability and specific activities toward glycol chitin and chitin hexasaccharide were significantly affected by the individual mutations. When *N*-acetylglucosamine hexamer was hydrolyzed by the wild type, the β-anomer of the substrate was preferentially hydrolyzed, producing the trimer predominantly and the dimer and tetramer in lesser amounts. When the mutated enzymes were used instead of the wild type, the enzyme cleavage sites in the hexamer substrate were clearly shifted, and the β-anomer selectivity was eliminated. The mutation effects on the enzymatic activity and stability were much more substantial in W82A than in W72A, but surprisingly the effects of the W82A/W72A double mutation were intermediate between those of the two single mutations. A molecular dynamics simulation of the wild type and the Trp-mutated enzymes indicated that the 70–82 loop becomes more flexible upon mutation and the flexibility increases in the order of W72A, W72A/W82A and W82A. We conclude that Trp72 interacts with the sugar residue but Trp82 modulates the loop flexibility, which controls the protein stability and enzymatic properties. These tryptophan residues are likely to interact with each other, resulting in the non-additivity of mutational effects.

1. Introduction

Chitinases (EC 3.2.1.14) hydrolyze β-1,4-glycosidic linkages of the *N*-acetylglucosamine (GlcNAc) polysaccharide also known as chitin. These proteins have been grouped into two families, GH-18 and GH-19, based on their amino acid sequences [1]. The enzymes of the individual families do not share sequence similarity and have completely different folds in their three-dimensional structures [2]. Among all of the chitinases, the first three-dimensional structure that was determined was that of 26 kDa endochitinase from barley seeds belonging to family GH-19 [3,4]. However, the structure–function relationship of the barley chitinase is still not well understood, as compared with family GH-18 chitinases, such as the enzymes from *Serratia marcescens* [5–8]. Part of the problem of slow progress in understanding the structure–function relationship of the barley chitinase is ascribed to the failure to obtain a crystal of the barley chitinase complexed with its oligosaccharide substrate. Thus, at present, we have been studying the structure and function of the barley chitinase primarily by means of site-directed mutagenesis and theoretical analyses of its protein structure [9,10].

The participation of aromatic side chains including tryptophan residues in chitinase–substrate interactions has been reported by Watanabe and his coworkers [11–14]. Hydrophobic and stacking interactions of the side chains make strong contacts with the substrate sugar residues. Such experimental evidence was obtained by X-ray crystallography and site-directed mutagenesis using several GH-18 enzymes. On the other hand, the crystal structure of a bacterial GH-19 chitinase from *Streptomyces coelicolor* A3(2) provided insight into the interactions of family GH-19 enzymes with their substrates [15]. The *Streptomyces* chitinase was reported to possess four subsites from −2 to +2, whereas the barley chitinase has six subsites from −3 to +3 [16]. A comparison of the crystal structures between the two GH-19 enzymes suggested the importance of Trp72, located in the loop consisting of residues 70–82 (70–82 loop) for the sugar residue interaction at +3/4 subsite of the barley enzyme [15]. In fact, as shown in Fig. 1, Trp72 is

Abbreviations: GH, glycosyl hydrolase; GlcNAc, 2-acetamido-2-deoxy-D-glucopyranose; $(GlcNAc)_n$, β-1, 4-linked oligosaccharide of GlcNAc with a polymerization degree of *n*; SDS-PAGE, sodium dodecyl sulfate-polyacrylamide gel electrophoresis; HPLC, high performance liquid chromatography; MSD, mean square displacement

* Corresponding author. Tel.: +81 742 43 8237; fax: +81 742 43 8976.
E-mail address: fukamizo@nara.kindai.ac.jp (T. Fukamizo).

1570-9639/$ – see front matter © 2009 Elsevier B.V. All rights reserved.
doi:10.1016/j.bbapap.2009.03.009

located at the surface of +3/4 subsite of the substrate binding cleft. Trp82 is buried inside the hydrophobic region, but the two tryptophan side chains are likely to interact with each other (Fig. 1B). It is of interest to examine the roles of these two tryptophan residues (+3/4 subsite) in the enzyme function. More recently, the crystal structure of a papaya family GH-19 chitinase complexed with two GlcNAc molecules was solved, which gave some insight into substrate interactions [17]. However, in this case, the two GlcNAc molecules bound to the −2 and +1 subsites, respectively, hence the function of the +3/4 subsite is still ambiguous. Mutation studies are needed to clarify the role of the +3/4 subsite of the substrate binding cleft of the family 19 chitinase from barley seeds.

Family GH-19 chitinases catalyze hydrolysis via an inverting mechanism [2]; that is, the enzymes produce an α-anomer from hydrolysis of β-1,4-glycosidic linkages. The mechanism has been confirmed by chromatographic analysis of the enzymatic products using a partition HPLC method, which resolves α- and β-anomeric forms of the individual GlcNAc oligosaccharides [18,19]. This type of HPLC analysis provides additional information about the anomeric selectivity of the sugar residue interactions at individual subsites. For example, a family GH-19 chitinase from *Vibrio proteolyticus* was found to preferentially hydrolyze the α-anomer of chitooligosaccharides, producing a reducing end disaccharide [20]. This means that the +2 subsite of this enzyme, which interacts with the reducing end residue of the oligosaccharide substrate, preferentially recognizes and binds the reducing end residue in its α-anomeric form. Thus, HPLC analysis provides useful information concerning anomeric recognition at a specific subsite.

In the present study, we mutated Trp72 and Trp82 localized to the 70–82 loop of a GH-19 endochitinase from barley seeds, and the mutated enzymes were characterized with respect to their stability, activity, mode of action, and anomeric selectivity. Furthermore, molecular dynamics simulations were performed to structurally rationalize the experimental data.

2. Materials and methods

2.1. Materials

Oligonucleotide primers for PCR and sequencing were purchased from SAWADY Co. All reagents for *Escherichia coli* cultivation and enzyme production were purchased from Wako Pure Chemical Co. and Nakalai tesque Co. Restriction enzymes for gene manipulations were from TOYOBO and Nippon Gene Co. Macro-Prep CM Support and Bio-Gel A-0.5 m used for enzyme purification were the products of Bio-Rad Lab. The glycol chitin used for the enzyme assay was prepared with the method of Yamada and Imoto [21]. *N*-acetylglucosamine oligosaccharides [$(GlcNAc)_n$ $n=2, 3, 4, 5$, and 6] were purchased from Seikagaku Kogyo Co. Other reagents were of analytical grade commercially available.

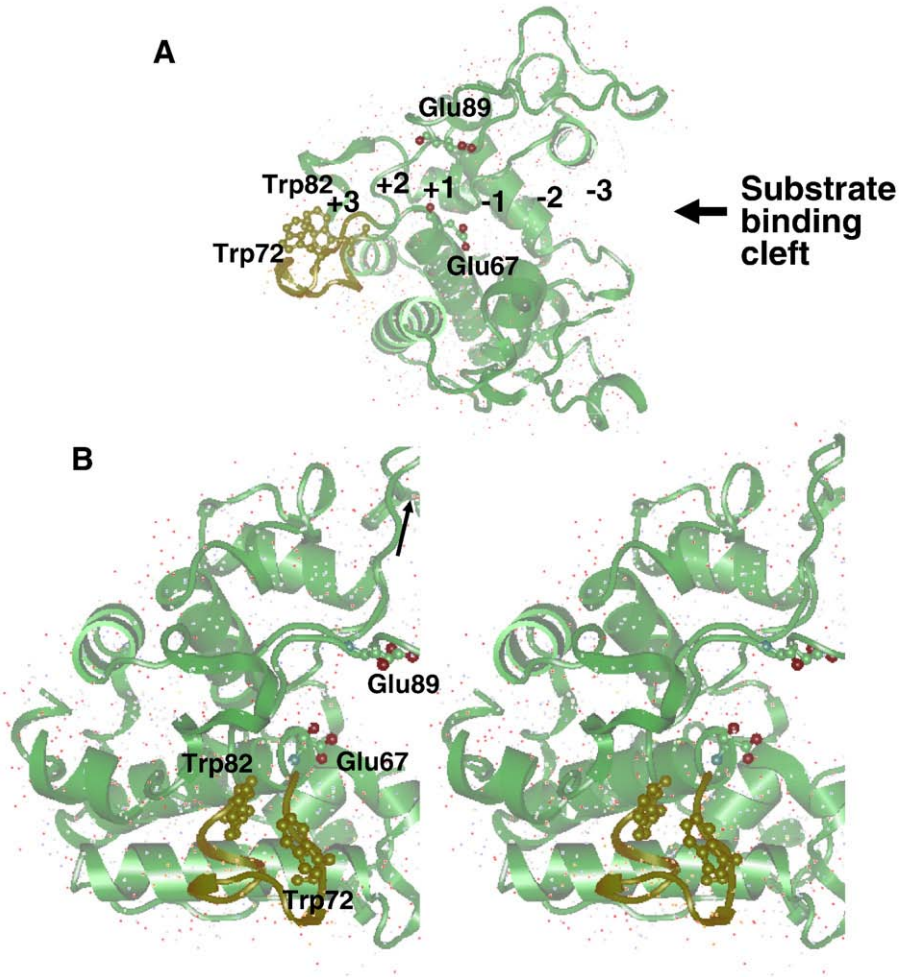

Fig. 1. Crystal structure of a family GH-19 endochitinase from barley seeds. Glu67 and Glu89 are the catalytic residues. Trp72 and Trp82 are located at +3/4 subsite of the substrate binding cleft, and the mutation targets in this study. The 70–82 loop is colored by dark green. The numbers indicate the putative subsites of the enzyme. (A) the entire protein structure. (B) stereoviews from the tryptophans' side.

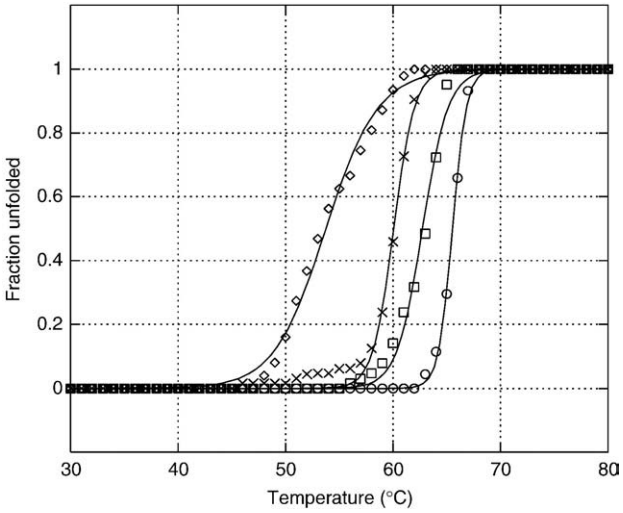

Fig. 2. Thermal unfolding curves of the wild type and the Trp-mutated endochitinases as determined by CD. The measurements were performed in 50 mM sodium acetate buffer pH 5.0. Protein concentrations were 2 μM. ○, wild type; □, W72A; x, W72A/W82A; ◊, W82A.

2.2. Enzyme production and purification

The *E. coli* expression vector of the barley chitinase reported previously [9] was transformed into *E. coli* Origami (DE3)pLysS, which was then grown to $OD_{600} = 0.6$ at 37 °C before induction with 0.1 mM isopropyl β-D-thiogalactopyranoside (IPTG). After induction, growth was allowed to continue for 3 h at 37 °C with shaking at 140 rpm. The cells were harvested by centrifugation at 5000 rpm for 10 min at 4 °C and then lysed with sonication according to the method previously reported [9]. Insoluble materials were removed by centrifugation at 15,000 rpm for 10 min at 4 °C, and the soluble fraction was dialyzed against 5 mM sodium phosphate buffer containing 10 mM NaCl (pH 7). Then, the dialyzed fraction was applied onto a cation exchange column of Macro-Prep CM Support (18×70 mm) equilibrated with the same buffer. After elution with the phosphate buffer, the chitinase fraction was eluted with a linear gradient elution of NaCl (from 10 to 200 mM). The chitinase active fractions were pooled and dialyzed against 50 mM sodium phosphate buffer at pH 7, applied to a gel-filtration column of Bio-Gel A-0.5 m, and then eluted with the same buffer. The chitinase preparation purified with gel-filtration was stored at 4 °C, and used for subsequent experiments.

2.3. Site-directed mutagenesis

Site-directed mutagenesis was performed using the QuickChange site-directed mutagenesis kit (Stratagene). We used 5′–GGACGGGGCCTTCGCCTGGGGCTACTGCTT–3′ (sense) and 5′–GGTGCAGTCGCCGCCCCGCCGGTGGTCTCG–3′ (antisense) for the production of W72A, 5′–GGACGGGGCCTTCGCCGCGGGCTACTGCTT–3′ (sense) and 5′–GGTGCAGTCGCCCACCCGCCGGTGGTCTCG–3′ (antisense) for W82A, and 5′–GGACGGGGCCTTCGCCGCGGGCTACTGCTT–3′ (sense) and 5′–GGTGCAGTCGCCGCCCCGCCGGTGGTCTCG–3′ (antisense) for W72A/W82A as the mutagenic primers. Individual mutations were confirmed by DNA sequencing using an automated DNA sequencer (ABI310A, Applied Biosystems).

2.4. Protein concentration

Protein concentrations were determined by their ultraviolet absorption at 280 nm using the extinction coefficients calculated from the equation reported by Pace et al. [22].

2.5. Electrophoresis of protein

SDS-polyacrylamide gel electrophoresis was performed according to the method of Laemmli [23] using an Amersham Low Molecular Weight Calibration Kit (GE Healthcare) as the standard. Protein bands were detected by staining with Coomassie brilliant blue R-250.

2.6. Enzyme assay

Chitinase activity was determined using glycol chitin as the substrate. Two microliters of enzyme solution were added to 0.5 ml of 0.5% glycol chitin in 50 mM sodium acetate buffer (pH 5), and the reaction mixture was incubated for 15 min at 37 °C. The reducing sugar generated by hydrolysis of the substrate was measured using the modified Schales' procedure [24].

2.7. Circular dichroism (CD)

Chitinase preparations were dialyzed against 50 mM sodium acetate buffer, pH 5. CD spectra were recorded using a Jasco J-720 spectropolarimeter (cell length, 0.2 cm).

2.8. Thermal unfolding

To obtain the thermal unfolding curve of the enzyme protein, the CD value at 222 nm was monitored, while the solution temperature was raised at a rate of 1°C/min by a temperature controller (PTC-423L, Jasco). To facilitate comparison between unfolding curves, the experimental data were normalized as follows. The fraction of unfolded protein at each temperature was calculated from the CD value by linearly extrapolating the pre- and post-transition baselines into the transition zone, and plotted against the temperature. Assays were performed in duplicate. Thermodynamic parameters could not be obtained, because of the poor reversibility of the unfolding transition.

2.9. HPLC determination of enzymatic products

Chitin hexasaccharide substrate was dissolved in 50 mM sodium acetate buffer, pH 5, and several microliters of the chitinase solution dialyzed against the same buffer were added to 100 μl of the substrate

Table 1
Effect of Trp mutations on the stability, enzymatic activity, and the 70–82 loop flexibility.

Protein	T_m[a] (°C)	ΔT_m (°C)	Glycol chitin		GlcNAc hexasaccharide		Mean square displacement[c] (nm^2)
			Specific activity (μmol/min/mg)	Relative activities (%)	Specific activities (mM/min/mg)	Relative activities (%)	
Wild type	65.5	0	6.31	100	139	100	9.2
W72A	62.7	−2.8	2.53	40.1	251	181	8.3
W82A	53.8	−11.7	0.02	0.3	23.4	16.8	18.2
W72A/82A	60.0	−5.5	0.38	6.0	n.d.[b]	n.d.[a]	13.2

[a] Values are calculated from the major transition zones of the unfolding curves shown in Fig. 2.
[b] n.d.: The values were not determined, because of the nonlinearity of the hydrolysis curves (Fig. 3). Nonetheless, the specific activity appears to be strongly enhanced.
[c] Mean square displacements (nm squared) were calculated from the structures obtained by molecular dynamics simulation.

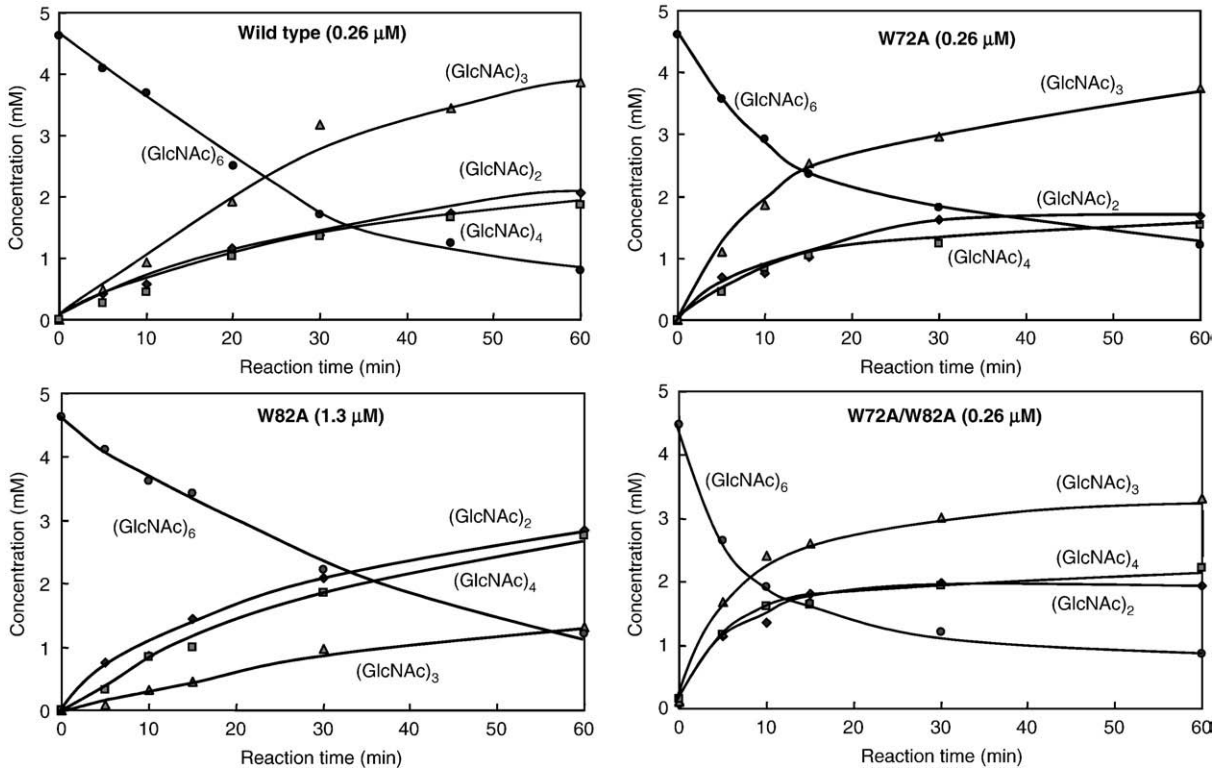

Fig. 3. Time-courses of $(GlcNAc)_6$ hydrolysis catalyzed by the wild type and the Trp-mutated endochitinases. The reaction mixture was incubated in 50 mM sodium acetate buffer pH 5 at 40 °C. ♦, $(GlcNAc)_2$; ▲, $(GlcNAc)_3$; ■, $(GlcNAc)_4$; ●, $(GlcNAc)_6$. Enzyme concentrations are listed in the individual figures.

solution. The final concentrations of the enzymes were 0.26 μM for wild type, W72A, and W72A/W82A and 1.3 μM for W82A. The substrate concentration was 4.6 mM. After incubating the reaction mixture at 40 °C for an appropriate period, a portion of the reaction mixture was withdrawn and mixed with the same volume of 0.5 M sodium hydroxide solution to completely terminate the enzymatic reaction. The resultant solution was applied onto a gel-filtration column of TSK-GEL G2000PW (7.5 × 600 mm, Tosoh) to quantitatively determine the substrate and product oligosaccharides. The elution was conducted with distilled water at a flow rate of 0.3 ml/min, and the oligosaccharides were monitored by absorption at 220 nm. From the peak area obtained by HPLC, oligosaccharide concentrations at each reaction time were calculated using the standard curve obtained with authentic saccharide solutions, and were plotted against the reaction time. When determining the α/β ratio of the hydrolytic products, the reaction mixture was incubated at the lower temperature (25 °C) to suppress mutarotation. After a given incubation period, a portion of the reaction mixture was withdrawn, and immediately applied onto a column of TSK-GEL Amide-80 (4.6 × 250 mm, Tosoh). The elution was conducted with 70% acetonitrile at a flow rate of 0.7 ml/min, and the detection was done as described above.

2.10. Molecular dynamics simulation

Mutations of the barley chitinase structure (PDB entry code: 2baa) were prepared with the aid of Swiss-PdbViewer 3.7 [25]. Subsequent energy minimizations and molecular dynamics studies of the proteins in water were carried out with the Gromacs 3.0.5 package [26,27]. The total length of each simulation was 10 ns. The simulation box was the truncated dodecahedron and it contained the protein solvated in single point charge (SPC) water molecules at charge-neutral physiological ion concentration [28]. Dummy hydrogen atoms were used. Weak temperature coupling (300 K) and pressure coupling (1.0 bar) were employed with coupling constants of 1.0 ps [29]. Coulomb interactions were calculated using the fast particle mesh Ewald summation technique (PME) with a grid spacing of 0.12 nm and a fourth order interpolation. The LINCS algorithm was used to constrain the bonds [30]. The center of mass motion was removed at each step. The system was energy minimized, followed by a short (10 ps) position restraining run for further equilibration. 10 ns MD simulations were completed at the Brutus Cluster at the Department of Biochemistry at the University of Oulu.

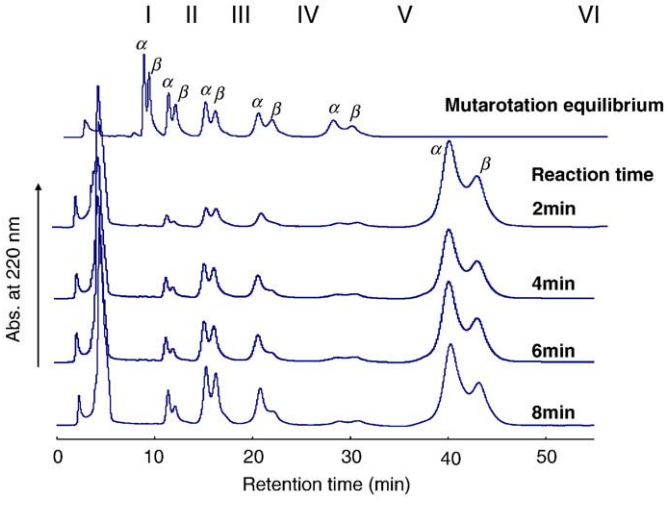

Fig. 4. Time-dependent HPLC profiles showing $(GlcNAc)_6$ hydrolysis by the wild type endochitinase. The reaction conditions were the same as in Fig. 3, except that the enzymatic reaction was conducted at 25 °C. HPLC separation was conducted by a TSK-GEL Amide-80 (4.6 × 250 mm, Tosoh) chromatography as described in Materials and methods. The flow rate was 0.7 ml/min. The top chromatogram was obtained by analyzing the aqueous solution of chitin oligosaccharide mixture (monomer to pentamer) equilibrated for mutarotation. The roman numerals indicate the polymerization degree of the chitin oligosaccharides.

3. Results

3.1. Production and purification of Trp-mutated chitinases

We successfully constructed plasmids containing the mutated barley chitinase genes, *HvChiW72A*, *HvChiW82A*, and *HvChiW72A/W82A*, which were then transformed into *E. coli* Origami (DE3)pLysS. Expression of the mutated enzymes was as efficient as that of the wild type enzyme, hence sufficient amounts of the mutated enzymes were purified by the procedure reported previously [10]. Each enzyme preparation was confirmed to exhibit a single band on SDS-PAGE (data not shown). CD spectra were determined to examine the mutation effects on the global conformation of the enzyme protein. The spectra of the mutant enzymes were almost identical to that of the wild type (data not shown), indicating that the secondary structures and global conformations are not significantly affected by the individual mutations.

3.2. Thermal stability

Fig. 2 shows the thermal unfolding curves determined by CD spectroscopy. Each unfolding curve exhibited a simple two-state transition, except during the initial stage of the unfolding transitions. It appears that a minor and unstable region unfolded at first, followed by the unfolding transition of the major stable region. Since the unfolding transitions were found to be irreversible, we could not determine the thermodynamic parameters and therefore evaluated the structural stability only from the transition temperatures (T_m) of the major transition zones. The Trp72 mutation lowered the T_m value from 65.5 °C (wild type) to 62.7 °C ($\Delta T_m = -2.8$ °C), while the Trp82 mutation lowered it to 53.8 °C ($\Delta T_m = -11.7$ °C). However, the T_m value for the double mutant W72A/W82A was 60.0, unexpectedly, and the ΔT_m value was only −5.5 °C. The effect of the double mutation on the protein stability was not additive; the effect was much lower than the sum of the effects of the individual single mutations. These data are summarized in Table 1.

3.3. Enzymatic activities of the mutated enzymes

The enzymatic activities of the three types of mutants were evaluated from the initial velocity of reducing sugar production from glycol chitin hydrolysis and are listed in Table 1. All of the three mutations significantly affected the enzymatic activity. The most remarkable effect was observed in W82A, which possesses 0.3% activity of that of the wild type. The relative activity of the double mutant W72A/W82A was intermediate of those of W72A and W82A. The mutation effects on the activity were almost parallel to those on protein stability (Table 1). The specific activities were also evaluated from the initial velocities of $(GlcNAc)_6$ hydrolysis, which was monitored by gel-filtration HPLC. The time-course profiles are shown in Fig. 3. The specific activity was enhanced by 1.8-fold by the W72A mutation. For W72A/W82A, specific activity toward $(GlcNAc)_6$ could not be accurately determined, because the hydrolysis curve of $(GlcNAc)_6$ did not exhibit sufficient linearity for activity determination. Nevertheless, it appears that the activity toward the oligosaccharide substrate was enhanced by the double mutation. A considerable decrease in enzymatic activity was observed only for W82A, of which the relative activity was only 17% of that of the wild type enzyme.

3.4. Cleavage specificity of N-acetylglucosamine hexasaccharide [$(GlcNAc)_6$]

To examine the cleavage specificity, product distributions obtained from the $(GlcNAc)_6$ substrate were compared between the wild type and the three mutated enzymes (Fig. 3). The wild type enzyme produced $(GlcNAc)_3$ predominantly, and $(GlcNAc)_2$ and $(GlcNAc)_4$ in lesser amounts. A similar product distribution was observed for W72A. These two enzymes hydrolyzed $(GlcNAc)_6$ into $(GlcNAc)_3 + (GlcNAc)_3$, and into either $(GlcNAc)_4 + (GlcNAc)_2$ or $(GlcNAc)_2 + (GlcNAc)_4$. Time-dependent HPLC profiles showing the productions of α- and β-anomers are shown in Figs. 4 and 5. The barley chitinase is an inverting enzyme; hence the newly produced reducing ends are α-anomeric [31], while the reducing ends originating from the substrate itself remain in mutarotation equilibrium. For both $(GlcNAc)_2$ and $(GlcNAc)_4$ products obtained from the wild type, the α/β ratios determined from the individual peak areas were 2.35 and 3.03 at 2 min of the reaction time, respectively, and higher than those at equilibrium (1.50), indicating that the frequency of cleavage into $(GlcNAc)_4 + (GlcNAc)_2$ is slightly higher than that into $(GlcNAc)_2 + (GlcNAc)_4$. In other words, the amount of $(GlcNAc)_6$ bound to −4 to +2 subsites (mode A) is slightly larger than that bound to −2 to +4 subsites (mode C), as shown in Fig. 6. When the W72A enzyme was used instead of the wild type, α/β values of $(GlcNAc)_2$ and $(GlcNAc)_4$ were 1.36 and 2.85 at 2 min of the reaction time, respectively. Since the α/β value of $(GlcNAc)_2$ was lower than that of the wild type, the relative amount of binding mode C appeared to decrease in W72A. For W82A, however, the production of $(GlcNAc)_2$ and $(GlcNAc)_4$ was strongly enhanced, whereas $(GlcNAc)_3$ production was suppressed (Fig. 3). An intermediate effect was observed for W72A/W82A; the

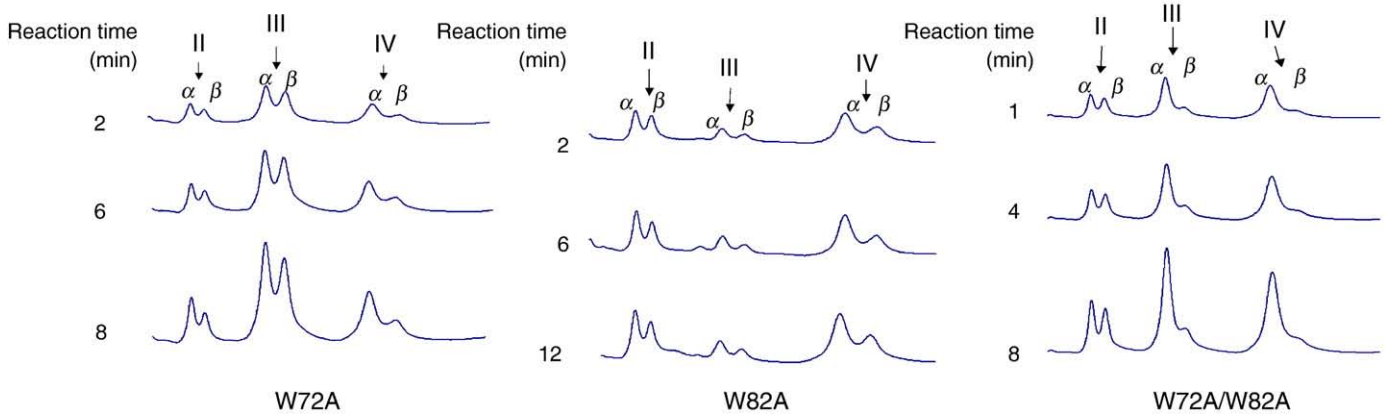

Fig. 5. Time-dependent HPLC profiles showing $(GlcNAc)_6$ hydrolysis by the Trp-mutated endochitinases. The reaction and HPLC conditions were the same as in Fig. 3, except that the enzymatic reaction was conducted at 25 °C. The roman numerals indicate the polymerization degree of the products.

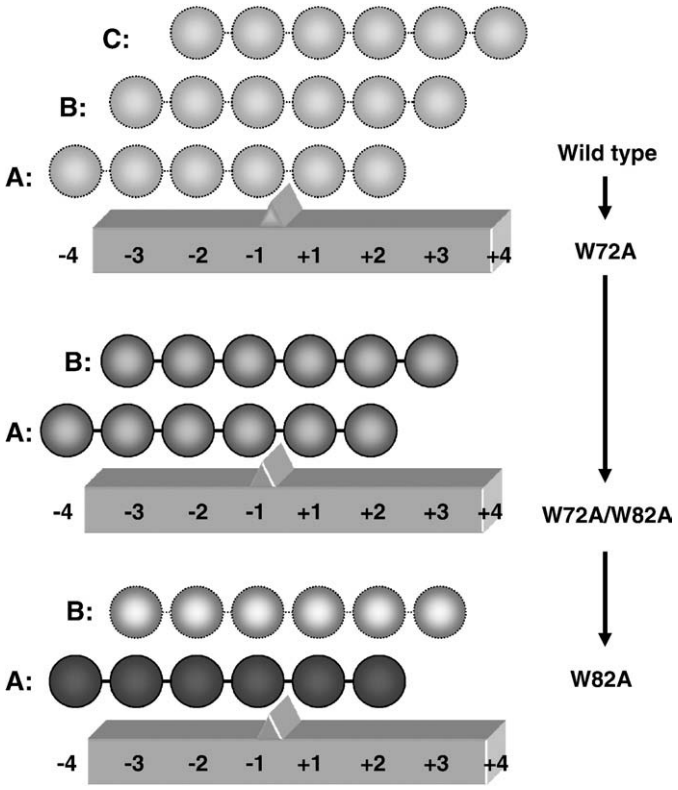

Fig. 6. Binding modes of $(GlcNAc)_6$ to barley endochitinases. The density of the shadow of the circles reflects the population estimated from the product distributions obtained by HPLC profiles shown in Figs. 3–5. The substrate binding cleft was assumed to consist of six subsites from −3 to +3, but −4 and +4 subsites are also indicated as putative subsites.

production of $(GlcNAc)_2$ and $(GlcNAc)_4$ was relatively enhanced in this double mutant enzyme (Fig. 3). In addition, the α/β values of $(GlcNAc)_4$ were 2.67 for W82A (2 min of the reaction time) and 4.10 for W72A/W82A (1 min of the reaction time), whereas the α/β values of $(GlcNAc)_2$ were 1.22 and 1.14, respectively, and rather lower than that at equilibrium (Fig. 5). These data indicate that binding mode C hardly occurs in W82A and W72A/W82A. It is clear that binding mode A is predominant in W82A and binding modes A and B are comparable in W72A/W82A, as shown in Fig. 6. The lower α/β ratio of $(GlcNAc)_2$ observed in W82A and W72A/W82A might have been derived from the β-anomeric selectivity at +2 subsite.

3.5. Anomeric selectivity in (GlcNAc)6 hydrolysis

For the $(GlcNAc)_3$ product from the wild type enzyme, the α/β value was 1.06 at 2 min of the reaction time; the amount of α-anomer was almost identical to that of β-anomer. This was due to the β-anomeric selectivity at the +3 subsite of the enzyme. As shown in the top of Fig. 7, when $(GlcNAc)_6$ binds to the subsites from −3 to +3, the +3 subsite selectively binds the β-anomer of the substrate, producing $(GlcNAc)_3$-α and $(GlcNAc)_3$-β. This situation brings about the identical peak areas of $(GlcNAc)_3$-α and $(GlcNAc)_3$-β. In fact, 48% of $(GlcNAc)_6$-β were hydrolyzed at 8 min, whereas only 33% of $(GlcNAc)_6$-α were hydrolyzed at the identical reaction time, as calculated from the corresponding peak areas shown in Fig. 4. For W72A, the α/β ratio of $(GlcNAc)_3$ was 1.09 at 2 min, and similar to that for the wild type enzyme (Fig. 5). Thus, the β-anomer is preferentially hydrolyzed even with W72A. However, α/β ratio of $(GlcNAc)_3$ was enhanced in W82A (2.16 at 2 min) and W72A/W82A (4.46 at 1 min), and the enhancement was more substantial in W72A/W82A. Obviously, β-anomeric selectivity at the +3 subsite is eliminated in W82A and W72A/W82A (Fig. 7). The much larger α/β ratio observed in W72A/W82A suggests that α-anomeric hexamer is preferentially hydrolyzed in the double mutant W72A/W82A.

3.6. Molecular dynamics simulation

Molecular dynamics simulations for the wild type and the Trp-mutated chitinases were conducted to examine the dynamics of the individual chitinase structures. From the 2D projection of trajectories (data not shown), the dynamical system was found to transfer from a starting conformation to another in a stable region, as was also observed from the energies of the protein systems, which in all cases converged to stable values. Thus, these observations confirm that the simulations resulted in sufficiently stable structures under the simulation conditions. As seen in the simulated structures for the wild type enzyme shown in Fig. 8, most secondary structures were not very flexible, but a great flexibility was observed in the 70–82 loop comprising Trp72 and Trp82, which tended to move toward the 20–26 residue loop (10 ns structure). Superposition of the simulated structures for the wild type and the mutated chitinases at 10 ns is shown in Fig. 9. Fig. 9A shows the entire protein structures, and the close-up view of the 70–82 residue loop is shown in Fig. 9B. Fig. 9C was obtained by rotating the structures in Fig. 9B by about 90°. The 70–82 loop in W72A (green chain) moved to the right side compared with the wild type (red chain) as shown in Fig. 9C. In W82A and W72A/W82A (blue and yellow chains, respectively), however, the 70–82 loop more intensively moved to the opposite direction (left side). In terms of dynamics, these results imply that each mutation causes a significant change in the dynamical modes of the native protein, such that each mutant eventually reaches a new stable structure. We

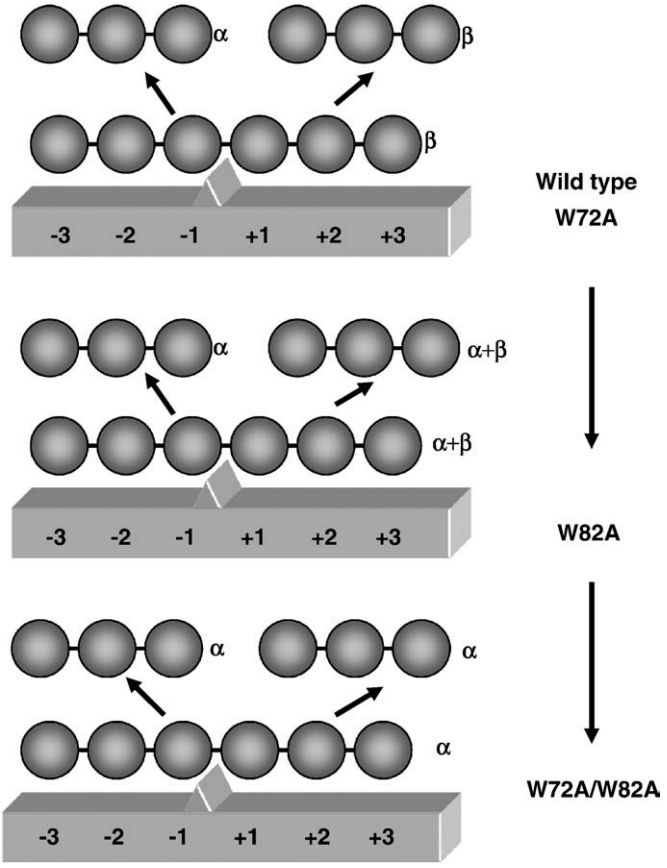

Fig. 7. Anomeric selectivity at the +3 subsite of the barley endochitinases. The selectivity was deduced from the α/β ratio of the $(GlcNAc)_3$ product shown in Figs. 4 and 5.

calculated the mean square displacement (MSD, a measure for extent of the structural change occurring in the course of the simulation with respect to the starting conformation) of the 70–82 loop based on the simulated structures. As listed in Table 1, the W82A mutant exhibited the highest flexibility (highest MSD) of the loop structure, while in W72A/W82A the flexibility was reduced compared with that in W82A, but greater than in wild type. W72A is comparable to the wild type with respect to the loop flexibility.

4. Discussion

Tryptophan residues are recognized to significantly participate in protein–carbohydrate interactions [32]. In family GH-18 chitinases, exposed tryptophan residues are aligned in the substrate binding cleft and are essential for binding and guiding the chitin chain into the substrate binding cleft [12,13]. Similarly, in family GH-19 chitinase from barley seeds, Trp72 was suggested to participate in substrate binding at the +3/4 subsite of the enzyme [15]. Trp82 is not exposed to the substrate binding surface but is located very close to Trp72, as shown in Fig. 1. Thus, we mutated these two tryptophan residues to examine their roles. Their thermal stabilities and specific activities toward the glycol chitin substrate were significantly reduced by the individual mutations, and the effects of the W72A, W72A/W82A, and W82A mutations increased in that order (Table 1). Nevertheless, the specific activities of W72A and W72A/W82A toward the hexasaccharide substrate were higher than that of the wild type, as listed in the table. This might result from substrate occupancy in the binding cleft; that is, the entire region of the binding cleft is occupied with the polysaccharide substrate, but not with the oligosaccharide substrate, which apparently forms significant amounts of nonproductive complexes with the enzyme. However, mutation of the residues localized to +3/4 subsite of the binding cleft might enhance the formation of productive complexes with the oligosaccharide substrates. This situation might bring about the enhanced specific activities of W72A and W72A/W82A toward the hexasaccharide substrate. Mizuno et al. [33] performed similar mutagenesis experiments using a family GH-19 chitinase from rice, and reported activity enhancement by a mutation of the corresponding loop structure. Data presented in this study for the barley chitinase are consistent with those reported for the rice enzyme.

The product distribution from the time-course of hexasaccharide hydrolysis catalyzed by W72A is very similar to that catalyzed by the wild type enzyme, as shown in Fig. 3. Nevertheless, the W72A mutation affected the α/β ratio of the $(GlcNAc)_2$ product (Fig. 5) and the specific activities as well (Table 1). As suggested by Hoell et al. [15], Trp72 interacts with the sugar residue at +3/4 subsite. The localization of Trp82 suggested that its side chain does not contact with the substrate sugar residue and is not responsible for substrate binding. However, dramatic decreases in the stability and activity were found in W82A. Furthermore, the product distribution obtained from the hexasaccharide hydrolysis catalyzed by W82A was considerably different from those of the wild type and the other mutant enzymes (Fig. 3); the relative amounts of $(GlcNAc)_2$ and $(GlcNAc)_4$ produced were much larger than those of the other enzymes. From the α/β ratios of these products shown in Fig. 5, $(GlcNAc)_6$ was estimated to predominantly bind to the subsites from −4 to +2 of W82A. The substrate binding mode was strongly shifted relative to that of the wild type enzyme. Trp72 is exposed to the solvent, while Trp82 is buried inside, as shown in Fig. 1. This situation would have resulted in the large difference in the mutational effects. The stronger effects of the W82A mutation on the stability, specific activity, and mode of action also suggest that this mutation results in a dramatic change in the conformation of the 70–82 loop of the enzyme, as discussed below.

We also found that the +3 subsite of the wild type enzyme specifically recognizes the β-anomer of the reducing end of the hexasaccharide substrate (Fig. 7). Honda et al. [20] examined the anomeric selectivity of a family GH-19 chitinase from *Vibrio proteolyticus* and reported that the enzyme recognizes the α-anomer of the oligosaccharide substrate. Although the two chitinases belong to the same GH family, the enzymes differ from each other in their specificity and mode of action. The *Vibrio* enzyme shows weak activity toward polymeric substrates and stronger activity toward chitooligosaccharide substrates. It hydrolyzes these substrates at the second

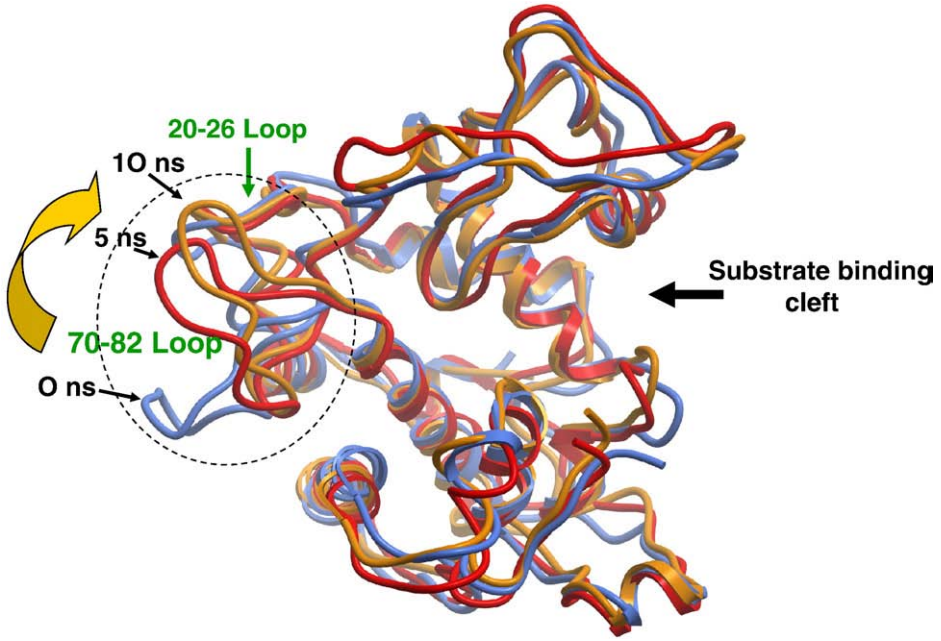

Fig. 8. Molecular dynamics simulation of the structure of wild type barley endochitinase. Individual traces are simulated structures at 0 (blue), 5 (red) and 10 (brown) ns, respectively. Most secondary structures were not very mobile, but the 70–82 residue loop was quite flexible. Calculation conditions were described in the text.

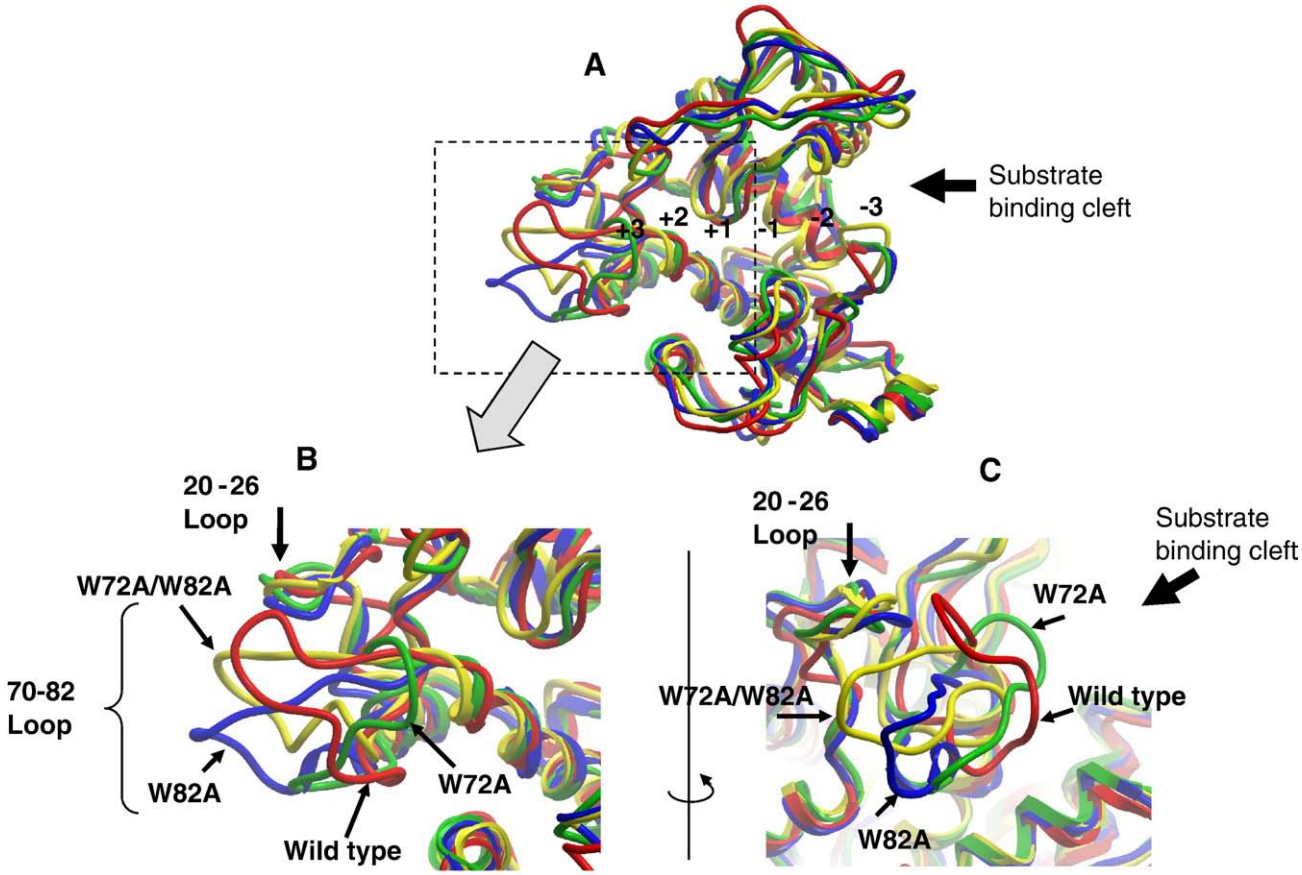

Fig. 9. Superposition of simulated structures of barley endochitinases at 10 ns. Individual traces are the simulated structures for the wild type (red), W72A (green), W82A (blue) and W72A/W82A (yellow). (A), the entire protein structures. (B), close-up view of the 70–82 residue loop, which was most flexible. (C), view obtained by rotating the (B) structure by about 90. Calculation conditions were described in the text.

linkage position from the reducing end. Thus, the +2 subsite of the *Vibrio* enzyme always interacts with the reducing end of the substrate. On the other hand, the barley chitinase examined in this study efficiently hydrolyzes the polymeric substrate with an endo-splitting mode. In this case, the polymeric substrate occupies the entire region of the binding cleft; hence all subsites in the binding cleft recognize internal sugar residues linked with each other through β-1,4-linkages. Therefore, +3 subsite of the enzyme recognizes only the β-anomeric substrate, which is preferentially hydrolyzed by the barley chitinase. However, the double mutant W72A/W82A exhibited preference of α-anomer to β-anomer, as shown in Fig. 7. This is the first report for inversion of the anomer selectivity of a specific subsite by mutagenesis. The double mutation might considerably alter the 70–82 loop conformation resulting in the inversion of the anomer selectivity at +3 subsite.

The most surprising result in this study is that the effect of the double mutation of Trp72 and Trp82 is smaller than that of the single mutation of Trp82. As described above, the drastic changes in the stability, activity, mode of action, and anomeric selectivity of W82A might be due to the conformational changes of the 70–82 loop induced by the W82A mutation. The loop flexibility might be an important factor bringing about the unexpected result obtained for W72A/W82A. Thus, molecular dynamics simulation of the wild type and Trp-mutated enzymes were performed to structurally rationalize the mutation effects on the stability, activity and mode of action. The simulation of the wild type enzyme revealed a considerable flexibility of the 70–82 loop comprising Trp72 and Trp82, as shown in Fig. 8. Superimposition of the simulated structures of the wild type and Trp-mutated enzymes at 10 ns suggested that the individual mutations affected the dynamical mode of the protein, especially at the 70–82 loop, triggering to transfer to a different conformation (Fig. 9). The individual mutations affect not only the dynamical modes but also MSD, as seen in Table 1. The MSD value was not enhanced by the W72A mutation, but enhanced by the other mutations (W82A and W72A/W82A). Interestingly, the enhancement was more intensive in W82A than in W72A/W82A. This mutation effect is almost parallel to those obtained from the stability, activity, mode of action, and anomer selectivity experiments. It is most likely that the effects of the tryptophan mutations on the various enzymatic properties are derived from the changes in the 70–82 loop's flexibility. Finally, we conclude that Trp72 interacts with the sugar residue at +3/4 subsite and that Trp82 modulates the loop flexibility, which strongly controls the protein stability and enzymatic properties. These tryptophan residues are likely to interact with each other, resulting in the non-additivity of mutational effects.

Acknowledgments

This work was supported by the “Academic Frontier” Project for Private Universities: a matching fund subsidy from MEXT, 2004-2008. We are grateful to Dr. Karl J. Kramer, U.S. Grain Marketing & Production Research Center, ARS-USDA, for his critical comments on the manuscript.

References

[1] B. Henrissat, Classification of chitinase modules, in: P. Jollès, R.A.A. Muzzarelli (Eds.), Chitin and Chitinases, Birkhäuser Verlag Basel/Switzerland, 1999, pp. 137–156.
[2] T. Fukamizo, Chitinolytic enzymes: catalysis, substrate binding, and their application, Curr. Protein and Peptide Sci. 1 (2000) 105–124.

[3] P.J. Hart, A.F. Monzingo, M.P. Ready, S.R. Ernst, J.D. Robertus, Crystal structure of an endochitinase from *Hordeum vulgare* L. seeds, J. Mol. Biol. 229 (1993) 189–193.
[4] P.J. Hart, H.D. Pfluger, A.F. Monzingo, T. Hollis, J.D. Robertus, The refined crystal structure of an endochitinase from *Hordeum vulgare* L. seeds at 1.8 A resolution, J. Mol. Biol. 248 (1995) 402–413.
[5] N.N. Aronson Jr, B.A. Halloran, M.F. Alexyev, L. Amable, J.D. Madura, L. Pasupulati, C. Worth, P. van Roey, Family 18 chitinase–oligosaccharide substrate interaction: subsite preference and anomer selectivity of *Serratia marcescens* chitinase A, Biochem. J. 376 (2003) 87–95.
[6] B. Synstad, S. Gåseidnes, D.M. van Aalten, G. Vriend, J.E. Nielsen, V.G. Eijsink, Mutational and computational analysis of the role of conserved residues in the active site of a family 18 chitinase, Eur. J. Biochem. 271 (2004) 253–262.
[7] G. Vaaje-Kolstad, D.R. Houston, F.V. Rao, M.G. Peter, B. Synstad, D.M. van Aalten, V.G. Eijsink, Structure of the D142N mutant of the family 18 chitinase ChiB from *Serratia marcescens* and its complex with allosamidin, Biochim. Biophys. Acta 1696 (2004) 103–111.
[8] S.J. Horn, P. Sikorski, J.B. Cederkvist, G. Vaaje-Kolstad, M. Sørlie, B. Synstad, G. Vriend, K.M. Vårum, V.G. Eijsink, Costs and benefits of processivity in enzymatic degradation of recalcitrant polysaccharides, Proc. Natl. Acad. Sci. U. S. A. 103 (2006) 18089–18094.
[9] M.D. Andersen, A. Jensen, J.D. Robertus, R. Leah, K. Skriver, Heterologous expression and characterization of wild-type and mutant forms of a 26 kDa endochitinase from barley (*Hordeum vulgare* L.), Biochem. J. 322 (1997) 815–822.
[10] T. Ohnishi, A.H. Juffer, M. Tamoi, K. Skriver, T. Fukamizo, 26 kDa endochitinase from barley seeds: an interaction of the ionizable side chains essential for catalysis, J. Biochem. 138 (2005) 553–562.
[11] T. Watanabe, A. Ishibashi, Y. Ariga, M. Hashimoto, N. Nikaidou, J. Sugiyama, T. Matsumoto, T. Nonaka, Trp122 and Trp134 on the surface of the catalytic domain are essential for crystalline chitin hydrolysis by *Bacillus circulans* chitinase A1, FEBS Lett. 494 (2001) 74–78.
[12] T. Uchiyama, F. Katouno, N. Nikaidou, T. Nonaka, J. Sugiyama, T. Watanabe, Roles of the exposed aromatic residues in crystalline chitin hydrolysis by chitinase A from *Serratia marcescens* 2170, J. Biol. Chem. 276 (2001) 41343–41349.
[13] T. Watanabe, Y. Ariga, U. Sato, T. Toratani, M. Hashimoto, N. Nikaidou, Y. Kezuka, T. Nonaka, J. Sugiyama, Aromatic residues within the substrate-binding cleft of *Bacillus circulans* chitinase A1 are essential for hydrolysis of crystalline chitin, Biochem. J. 376 (2003) 237–244.
[14] F. Katouno, M. Taguchi, K. Sakurai, T. Uchiyama, N. Nikaidou, T. Nonaka, J. Sugiyama, T. Watanabe, Importance of exposed aromatic residues in chitinase B from *Serratia marcescens* 2170 for crystalline chitin hydrolysis, J. Biochem. 136 (2004) 163–168.
[15] I.A. Hoell, B. Dalhus, E.B. Heggset, S.I. Aspmo, V.G. Eijsink, Crystal structure and enzymatic properties of a bacterial family 19 chitinase reveal differences from plant enzymes, FEBS J. 273 (2006) 4889–4900.
[16] Y. Honda, T. Fukamizo, Substrate binding subsites of chitinase from barley seeds and lysozyme from goose egg white, Biochim. Biophys. Acta 1388 (1998) 53–65.
[17] J. Huet, P. Rucktooa, B. Clantin, M. Azarkan, Y. Looze, V. Villeret, R. Wintjens, X-ray structure of papaya chitinase reveals the substrate binding mode of glycosyl hydrolase family 19 chitinases, Biochemistry 47 (2008) 8283–8291.
[18] M. Ueda, M. Kojima, T. Yoshikawa, N. Mitsuda, K. Araki, T. Kawaguchi, K. Miyatake, M. Arai, T. Fukamizo, A novel type of family 19 chitinase from *Aeromonas* sp. No.10S-24. Cloning, sequence, expression, and the enzymatic properties, Eur. J. Biochem. 270 (2003) 2513–2520.
[19] C. Sasaki, Y. Itoh, H. Takehara, S. Kuhara, T. Fukamizo, Family 19 chitinase from rice (*Oryza sativa* L.): substrate-binding subsites demonstrated by kinetic and molecular modeling studies, Plant Mol. Biol. 52 (2003) 43–52.
[20] Y. Honda, H. Taniguchi, M. Kitaoka, A reducing-end-acting chitinase from *Vibrio proteolyticus* belonging to glycoside hydrolase family 19, Appl. Microbiol. Biotechnol. 78 (2008) 627–634.
[21] H. Yamada, T. Imoto, A convenient synthesis of glycol chitin, a substrate of lysozyme, Carbohydr. Res. 92 (1981) 160–162.
[22] C.N. Pace, F. Vajidos, L. Fee, G. Grimsley, T. Gray, How to measure and predict the molar absorption coefficient of a protein, Protein Sci. 4 (1995) 2411–2423.
[23] U.K. Laemmli, Cleavage of structural proteins during the assembly of the head of bacteriophage T4, Nature 227 (1970) 680–685.
[24] T. Imoto, K. Yagishita, A simple activity measurement of lysozyme, Agric. Biol. Chem. 35 (1971) 1154–1156.
[25] N. Guex, M.C. Peitsch, SWISS-MODEL and the Swiss-PdbViewer: an environment for comparative protein modeling, Electrophoresis 18 (1997) 2714–2723.
[26] H.J.C. Berendsen, D. van der Spoel, R. van Drunen, A message-passing parallel molecular dynamics implementation, Comp. Phys. Comm. 91 (1995) 43–56.
[27] E. Lindahl, B. Hess, D. van der Spoel, GROMACS 3.0: a package for molecular simulation and trajectory analysis, J. Mol. Mod. 1 (2001) 306–317.
[28] H.J.C. Berendsen, J.P.M. Postma, W.F. van Gunsteren, J. Hermans, Interaction models for water in relation to protein hydration, in: B. Pullman (Ed.), Intermolecular Forces, Reidel, Dordrecht, 1981, pp. 331–342.
[29] H.J.C. Berendsen, J.P.M. Postma, A. DiNola, W.F. van Gunsteren, J.R. Haak, Molecular dynamics with coupling to an external bath, J. Chem. Phys. 181 (1984) 3684–3690.
[30] B. Hess, H. Bekker, H.J.C. Berendsen, J.G.E.M. Fraaije, LINCS: a linear constraint solver for molecular simulations, J. Comp. Chem. 18 (1997) 1463–1473.
[31] T. Hollis, Y. Honda, T. Fukamizo, E. Marcotte, P.J. Day, J.D. Robertus, Kinetic analysis of barley chitinase, Arch. Biochem. Biophys. 344 (1997) 335–342.
[32] N.K. Vyas, Atomic features of protein–carbohydrate interactions, Curr. Opin. Struct. Biol. 1 (1991) 732–740.
[33] R. Mizuno, T. Fukamizo, J. Sugiyama, Y. Nishizawa, Y. Kezuka, T. Nonaka, K. Suzuki, T. Watanabe, Role of the loop structure of the catalytic domain in rice class I chitinase, J. Biochem. 143 (2008) 487–495.